Effects of SbCl₅, Ethylamine, Imidazole and 2-Methylimidazole on Redox and Structural Behaviours of Manganese(III) *meso*-5,10,15,20-*tetrakis*(4-pyridyl)porphyrin

V. Thandiayyakone[1], A. Murugan[2,*], Ijaz Ullah Muzaddadi[2], Nabam Tayum[2], Nagendra Nath Yadav[2], Pranjit Saikia[2], T. Rajkumar[3], A. Manohar[4] and Mithun Chakrabarty[5]

[1]Research and Development Centre, Bharathiar University, Coimbatore-641046, India
[2]Department of Chemistry, North Eastern Regional Institute of Science & Technology, Nirjuli-791109, India
[3]Department of Chemistry, Rajah Serfoji Government College (Affiliated to Bharathidasan University), Thanjavur-613005, India
[4]Department of Chemistry, Periyar Maniammai Institute of Science and Technology, Periyar Nagar, Vallam, Thanjavur 613403, India
[5]Department of Chemistry, St. Anthony's College, Shillong-793001, India

*Corresponding author: E-mail: nspmmurugan@gmail.com

A porphyrin compound manganese(III) *meso*-5,10,15,20-*tetrakis*(4-pyridyl)porphyrin, Mn(Py)₄P containing manganese(III) and 4-pyridyl ligands was synthesized. The UV-visible spectrophotometry and cyclic voltammetry were used to investigate the axial ligand and the redox behaviours of Mn(Py)₄P. This study investigates the reduction properties of Mn(Py)₄P using primary amine, imidazole and 2-methylimidazole as axial ligands. Reduction of Mn(Py)₄P leads to a shift in absorption bands, indicating the conversion from manganese(III) to manganese(II) porphyrin. The addition of primary amine results in a square pyramidal structure for Mn(II) porphyrin, while imidazole or 2-methylimidazole leads to the formation of tetragonal complexes. These changes in geometry result in a decrease in π-bonding. The observed spectral patterns support the involvement of axial ligands in the 5th and 6th positions of manganese(III) porphyrin. The cyclic voltammogram confirmed the alteration in geometry, indicating changes in the redox properties of compound. As a whole, the results of this study provide light on the ways where the behaviour of in which Mn(Py)₄P can be altered by the presence of other molecules.

Keywords: Manganese, Porphyrin, Primary amine, Imidazole, 2-Methylimidazole, Redox behaviours.

INTRODUCTION

Porphyrins, which play a part in metabolism, are found in all forms of biological things. Hemes are a kind of porphyrins and their reduced or modified derivatives. Hemoglobins, myoglobins, cytochromes, catalases and peroxidases all include hemes. Hemes contain the binding metal iron and many chlorophylls and bacteriochlorophylls consist of magnesium [1]. In the ultraviolet (UV) wavelengths, where UV light is intensely absorbed by porphyrins and to a lesser extent in the long visible bands, changes to excited electronic states take place. Type I processes includes the excited porphyrin interacting with structures in biology, while type II processes involve a molecule of oxygen generating excited singlet oxygen. In addition to their well-known photodynamic action, porphyrins also exhibit a unique, light-independent function [2].

Porphyrin nanostructured' multipurpose characteristics have demonstrated the potential for improved phototherapy drug delivery using porphyrin-based active targeting because porphyrins exhibit excellent phytochemical properties, particularly the ability to produce singlet oxygen, which makes them a viable photodynamic therapy treatment candidate [3]. Infrared fluorescence imaging, PET-MRI dual-modality, PET-MRI and positron emission tomography (PET) can all use porphyrins to increase signals. Because of their unique chemical and physical characteristics, porphyrins can be used to detect and eliminate tumours [4]. The incorporation of imidazole and N-methylimidazole as axially ligated to the ruthenium centre was studied for the spectral and electrochemical properties of carbonyl ruthenium(II) *meso*-tetramesityl porphyrin Ru(CO)-(TMP), which showed an identical spectral and electrochemical capabilities. The higher variations in absorption wavelength,

the lower CO stretching frequency and the lower oxidation potential are indicative of the hydroxide anion's stronger capacity to coordinate, which leads to greater impacts on the ruthenium porphyrin. The production constants of the one- and two-electron oxidized ruthenium porphyrins are also higher for the ⁻OH anion than for the imidazole bases. The spectro-electrochemical experiments revealed that the first oxidation of six-coordinated ruthenium porphyrin complexes featured porphyrin ring oxidations, although hydroxide gives a significant amount of electron density to the ruthenium centres [5]. Using ceric ammonium nitrate as an oxidizer, the water-soluble zinc isoporphyrins have oxidized. Significant near-infrared peak absorption and reduced Soret band intensity can be seen in the electronic spectra of the synthetic isoporphyrins. The cyclic voltammograms of the isoporphyrins revealed one irreversible reduction at a very low potential and this result supported the use of reducing agents to convert zinc-isoporphyrin to parent porphyrin [6].

As single-site catalysts for the oxidation of water, a series of 5,10,15-*tris*(pentafluorophenyl)corrole [Co(tpfc)] derivatives with different axial ligands were investigated. The findings demonstrate that the catalytic oxygen evolution reaction (OER) activity is significantly influenced by the axial ligands on Co centres. In general, Co corroles with *trans*-axial ligands that donate electrons are more active than others. The strong trans effect, which weakens the Co(V)-oxo bond and lowers the activation energy barrier for the formation of the O-O bond by nucleophilic water attack on the Co(V)-oxo unit, could have been the cause of this improvement [7]. At normal temperatures, the triplet state of the oxidation of VOTPP can be detected in the EPR spectrum. This may imply that a_{1u} contains a sizable amount of unpaired spin density. The oxidation potentials of the vanadyl porphyrin are altered (shifted to higher positive potentials) by the electron-withdrawing substituents in the phenyl ring of the porphyrin [8]. In the cyclic voltammograms, redox peaks for the dimeric species of vanadyl *meso*-porphyrin dimethyl ester have been found at various concentration ranges. At low temperatures, the monomeric radical cation of VO(MESO) has been discovered and its triplet EPR spectrum is observed. In the monomeric radical cation of VO(MESO), a distance of 3.8 Å has been measured between the unpaired electron in the porphyrin ring and the d electron in the vanadium orbital. This outcome is explained as coming from the porphyrin's electron's a_{1u} ground state [9]. The oxidation at 0.0995 V of the ΔE value in the cyclic voltammogram of vanadyl *meso*-5,10,15,20-*tetrakis*(2,5-methoxyphenyl)porphyrin is indicative of a porphyrin mono-cation. The successive production of the mono-cation and di-cation radicals is well supported by the spectrum characteristics observed during the oxidation. According to VO *meso* porphyrin's EPR spectrum, it might be oxidized with SbCl₅ in dichloromethane to form the radical cation. At low temperatures, a radical cation can be observed and this spectrum is consistent with a monomeric radical cation [10]. According to the reviewed literature, there have been no prior investigations into the cyclic voltammetry and UV-visible spectrophotometry-based analyses of the axial ligand and the redox properties of Mn(Py)₄P, a manganese(III) *meso*-5,10,15,20-*tetrakis*(pyridyl)porphyrin.

The compounds, *meso*-5,10,15,20-*tetrakis*(4-pyridyl)-porphyrin (Py)₄P, tetra-*n*-butylammonium iodide (TBAI), imidazole and 2-methylimidazole were bought from Aldrich and utilized without additional purification. The primary amine utilized in dichloromethane was used as received from SRL Chemical, India. Before usage, dichloromethane supplied by SD Fine Chemicals was distilled after being refluxed over P₂O₅. Manganese(III) *meso*-5,10,15,20-*tetrakis*(pyridyl)porphyrin, Mn(Py)₄P has been synthesized according to the procedure proposed by Murugan *et al.* [11]. Tetra-*n*-butylammonium perchlorate (TBAP) was prepared by reacting tetra-*n*-butyl-ammonium iodide with sodium perchlorate and then recrystal-lizing the resulting compound from methanol.

The cyclic voltammetric measurements were done by CHI620B CH instrument at North-Eastern Hill University, Shillong, India. The visible spectrum in the 300-750 nm region was recorded using a Beckman 650DU spectrophotometer at North-Eastern Hill University, Shillong, India. The reduction properties of individual 0.05 mM primary amine drops added in a quartz cuvette and the axial ligand properties were analyzed.

RESULTS AND DISCUSSION

Cyclic voltammetric studies: Manganese(III) *meso*-5,10,15,20-*tetrakis*(4-pyridyl)porphyrin [Mn(Py)₄P] has an oxidation potential of 1.2155 V and a reduction potential of 1.1109 V concerning oxidation characteristics. At 0.4469 V, a new reduction potential has emerged. The corresponding ΔE value is 0.1046 V and the $E_{1/2}$ value is 1.1632 V (Fig. 1). The oxidation state of manganese in Mn(Py)₄P changes from +3 to +4 at 0.4469 V, while the ligand oxidizes at 1.2155 V. The formation of a dication radical is confirmed by the oxidation potential of 1.2155V. The electron-donating pyridyl group raises the density of electrons in the macrocycle of porphyrin system. The creation of manganese(IV) porphyrin ring structure directs
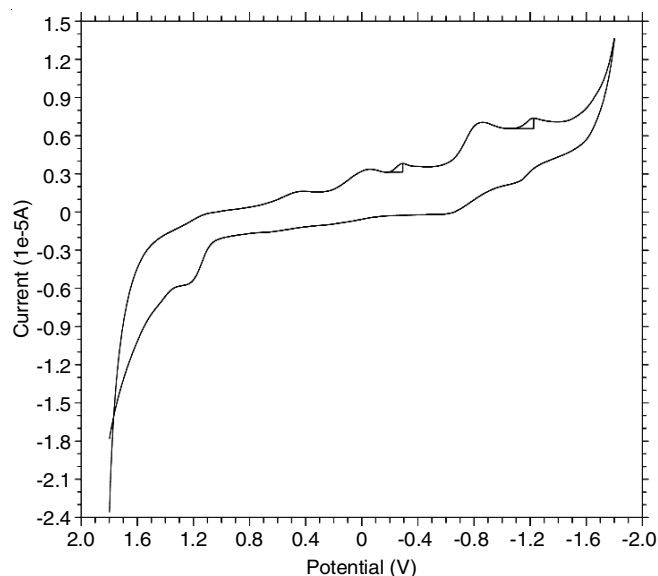

Fig. 1.   Cyclic voltammogram of the mixture of 0.5×10^{-3} M Mn(Py)₄P and 0.1 M TBAP in dichloromethane recorded at room temperature with a 0.01 V/s scan rate

that the core metal manganese(IV) ion's higher oxidation state authorizes a stabilizing impact [12]. Due to the occurrence of a one-electron reversible transfer, the anodic to cathodic peak current ratio (i_{pc}/i_{pa}) for the metal oxidations is equal to 1. Mn(III) *meso*-porphyrin is converted to manganese(IV) *meso*-porphyrin through one electron transfer, which requires a deformed pseudo-tetrahedral shape [13].

The Mn(Py)$_4$P possesses the oxidation potentials of -0.6144 and -1.1371 and reduction potentials of -0.8235 and -01.2208 in terms of reduction characteristics. Two additional reduction potentials have been observed, with the values of -0.0395 V and -0.2901 V. The ΔE values vary between 0.0837 V and 0.2091 V (Fig. 1). The values of $E_{1/2}$ are -0.7189 V and -1.1790 V. The anodic to cathodic peak current ratios for reductions are 0.9314 and 0.7461. The decreases in anodic to cathodic peak current ratios show that one electron transfer is a single transfer, but another is a quasi-irreversible transfer. The manganese(III) to manganese(II) porphyrin reduction process is demonstrated by the reduction peak at -0.2901 V, which occurs as a result of chloride ions from TBAP. This process results the formation of highly electron-rich porphyrin, which destabilizes the manganese(II) oxidation state [14].

Using TBAP as the supporting electrolyte, a cyclic voltammogram of Mn(III) porphyrin was captured in a dichloromethane solvent at a 0.06 V/s scan rate (Fig. 2). It exhibits one cathodic maximum at -0.5650 V as a result of manganese(III) being converted to manganese(II). The anodic side likewise displays a voltage at -0.4450 V that can be attributed to the oxidation of manganese(II) to manganese(III). The i_{pc}/i_{pa} ratio (0.7890) confirmed that these two peaks were nearly reversible with one another. Due to the reduction of the porphyrin ring system, this compound exhibits one irreversible peak at -1.2 V is also seen in the cyclic voltammogram of porphyrin ligand.
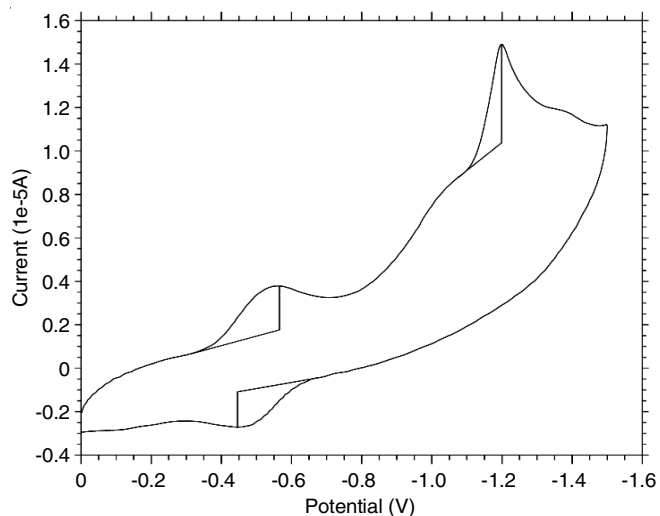

Fig. 2. Cyclic voltammogram of the mixture of 0.5 × 10^{-3} M Mn(Py)$_4$P and 0.1 M TBAP in dichloromethane recorded at room temperature with a 0.06 V/s scan rate

UV-visible spectral studies: The UV-visible spectra of Mn(Py)$_4$P with varying primary amine concentration (Fig. 3) was used to assess the reduction properties. The axial ligand
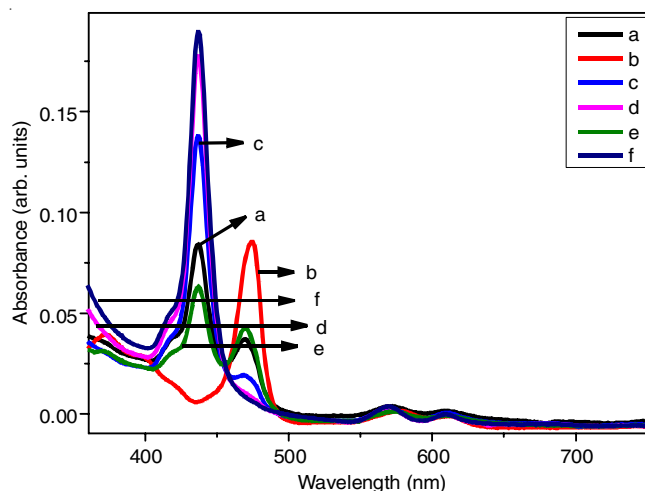

Fig. 3. UV-visible spectra of Mn(Py)$_4$P with varying primary amine concentrations in dichloromethane recorded at room temperature

properties of 10^{-5} M Mn(Py)$_4$P have been reported with ethylamine, diethylamine and triethylamine in earlier work. No changes have occurred after the addition of ethylamine [15]. In this work, reduction properties of 10^{-3} M Mn(Py)$_4$P has done through primary amine. Bathochromic shift of the split soret bands from 438 to 472 nm (Fig. 3b-d), hypochromic shift of two of the split soret bands lose intensity and hypsochromic shift of the Q band from 580 to 570 nm were observed. It shrinks as a result, proving that Mn(III) porphyrin can become Mn(II) porphyrin by shedding one electron.

When Mn(II) porphyrin is produced, it takes the shape of a high-spin d^5 configuration with the primary amine occupying the $d_{x^2-y^2}$ orbital at the fifth position. Because of the low $d_{x^2-y^2}$ orbital energy, Mn(II) is unlikely to be on the porphyrin's plane. Mn(II) porphyrin now has a square pyramidal structure as its form. Succeeding the accumulation of primary amine, Mn(II) porphyrin shows a typically visible spectrum, as shown in Fig. 3b-e. The fifth position in the Mn(II) porphyrin has engaged by one amine as the axial ligand, followed by mono-anion radicals through dianions radicals of Mn(II). A reduction in Mn(III)/Mn(II) is understood in the resulting spectra, consistent with the earlier report [16]. The regeneration of the typical Mn(III) spectra after reoxidation with SbCl$_5$ demonstrated that the product remained stable throughout the course of this experiment. This suggests that the compound switches from Mn^{3+} state, where there is a strong interaction between the four pyrrole N and metal that is calmed by the back donation from metal to ligand, to an Mn^{2+} state, where manganese metal-porphyrin bonding is not preferred and the spectra of Mn(II) are normal. These findings suggest that Mn(Py)$_4$P shape changes from octahedral to square pyramidal [17].

UV-visible spectra of Mn(Py)$_4$P with varying imidazole concentration depicted in Fig. 4 was used to assess the axial ligand properties, which illustrates the presence of three Soret bands at wavelengths of 374, 403 and 489 nm. However, the intensity of the absorption peak at 480 nm decreases due to the hypochromic effect. Furthermore, the intensity of the absorption peaks at 374 and 403 nm initially decreases due to the hypochromic effect and subsequently increases due to the
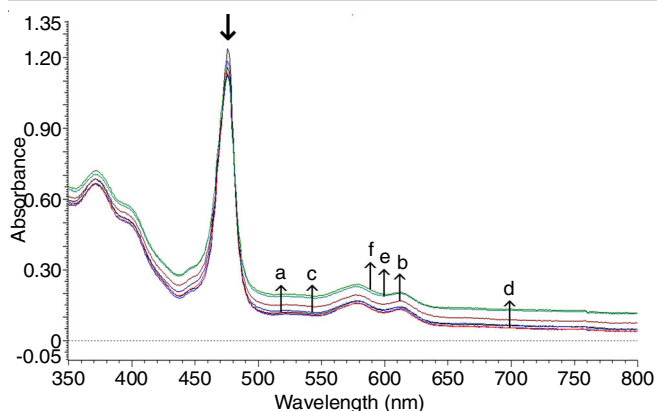
Fig. 4.   Absorption spectra of 10^{-3} M Mn(Py)$_4$P with varying imidazole concentration

hyperchromic effect. Similar observations are made at the Q bands, where the two peaks at 574 and 614 nm exhibit an initial decrease in intensity due to the hypochromic effect, followed by an increase due to the hyperchromic effect. No significant changes in the rest of the spectral pattern are observed.

The final spectral pattern indicates the presence of hexa-coordinated Mn(III) porphyrins, suggesting that two imidazole molecules occupy the 5th and 6th positions as axial ligands. This suggests that the formation of tetragonal complexes reduces π-bonding. This reduction may occur as a result of the expansion of the inplane metal of manganese in the porphyrin, allowing for the inclusion of two axial ligands positioned at a considerable distance from the manganese metal [18]. Therefore, the geometry of manganese(III) pyridyl porphyrin transforms from octahedral to tetragonal complexes, leading to a decrease in π-bonding with the successive addition of imidazole.

The axial ligand properties of Mn(Py)$_4$P were evaluated by analyzing the UV-visible spectra with varying concentrations of 2-methylimidazole as presented in Fig. 5. The spectra revealed three Soret bands at wavelengths of 366 nm, 400 nm and 465 nm. However, the absorption peak at 465 nm experiences a decrease in intensity due to the hypochromic effect. Similarly, the intensity of the other two Soret bands at 366 nm and 400 nm also decreases due to the hypochromic effect.
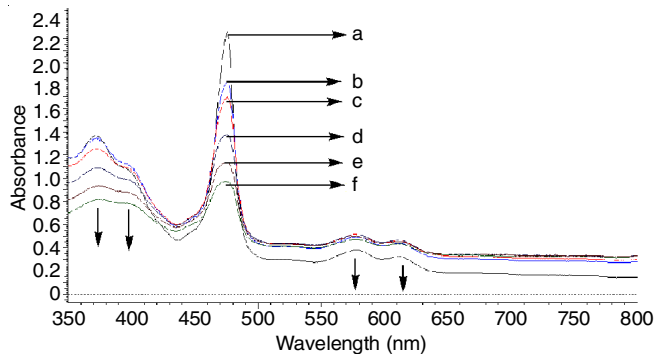

Fig. 5.   Absorption spectra of 10^{-3} M Mn(Py)$_4$P with varying 2-methyl-imidazole concentration

Observations at the Q bands indicate that initially, the two peaks at 578 nm and 610 nm increase in intensity due to the hyperchromic effect. However, with successive additions of

2-methylimidazole, these peaks ultimately decrease due to the hypochromic effect. No significant changes in the overall spectral pattern are observed. The final spectral pattern suggests the presence of six-coordinated manganese(III) porphyrins, indicating that two 2-methylimidazole molecules may occupy the 5th and 6th positions as axial ligands. Consequently, the formation of tetragonal complexes leads to a reduction in π-bonding. This reduction is likely attributed to the expansion of the in-plane metal of manganese in the porphyrin, enabling the inclusion of two axial ligands positioned at a significant distance from the manganese metal [18]. These findings suggest that the geometry of Mn(III) pyridyl porphyrin undergoes a transition from octahedral to tetragonal complexes, resulting in a decrease in π-bonding following successive additions of 2-methylimidazole.

Oxidation properties of Mn(Py)$_4$P: The absorption band of Mn(Py)$_4$P undergoes a shift towards longer wavelengths (red shift) and a decrease in peak intensity due to hypochromism, causing the band to move from 468 to 476 nm (Fig. 6). A point of isosbesticity is observed at 488 nm. This indicates that SbCl$_5$ coordinates with manganese metal as a result of the 5th and 6th locations in the manganese forming axial ligand coordination. Based on the CV data, the peaks are observed at 0.4469 V and 1.2155 V, which correspond to the oxidation of Mn(III) to Mn(IV) and Mn(IV) to Mn(V), respectively (**Scheme-I**) [19].
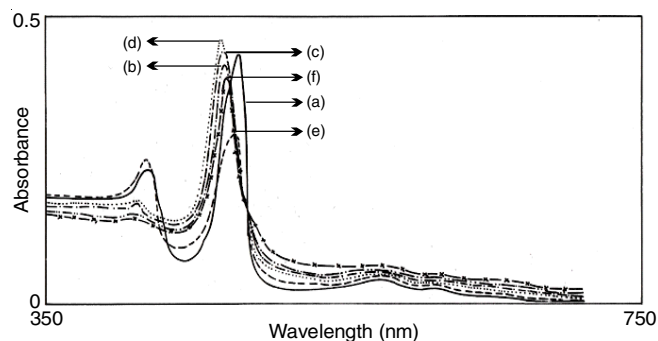

Fig. 6.   Absorption spectra of Mn(Py)$_4$P with varying SbCl$_5$ concentration in CH$_2$Cl$_2$ recorded at ambient temperature

The observed behaviour may suggest the presence of a spin isomerization equilibrium between the low-spin and ruffled complex and the high-spin and planar form. Factors that can affect this reaction include the electronic effects of peripheral or axial substituents of SbCl$_5$, the size of the coordination cavity, which can be decreased by the saturation of methylidene bridges or increased by the saturation of π-bonds between β-carbons, as well as the replacement of the methylidene bridge(s) by direct or aza bridge(s). Absorption spectroscopy results also indicate that the axial ligands of SbCl$_5$ and the porphyrin can greatly influence the redshifted absorption of Mn porphyrin [20].

Conclusion

The study of manganese(III) *meso*-5,10,15,20-*tetra-kis*(pyridyl)porphyrin, Mn(Py)$_4$P, using cyclic voltammetry and UV-visible spectrophotometry has provided valuable insights into its axial ligand and redox properties. Primary amine was
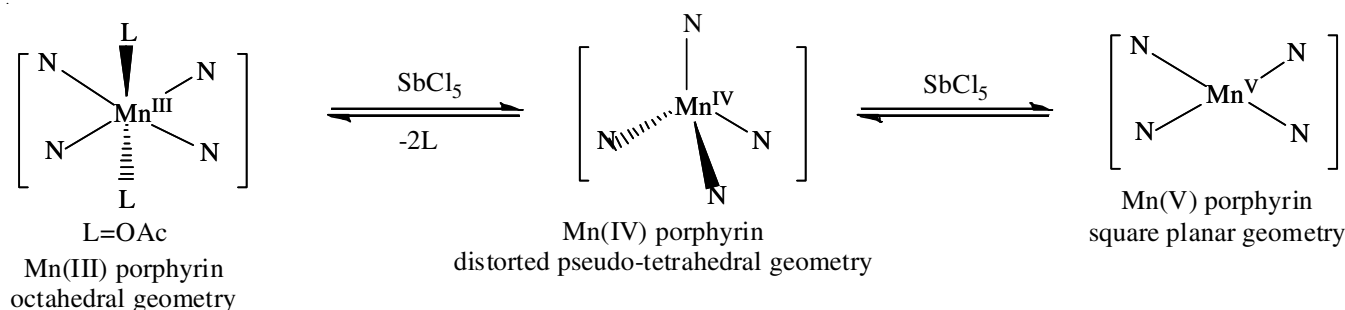
Scheme-I: Manganese(III) *meso* porphyrin converted to manganese(V) *meso* porphyrin through manganese(IV) *meso* porphyrin

used to reduce $Mn(Py)_4P$, resulting in a bathochromic shift in the split Soret bands and a hypsochromic shift in the Q band, indicating the conversion from Mn(III) to Mn(II) porphyrin. The addition of a primary amine caused a change in the axial ligand properties, transforming the octahedral geometry into a square pyramidal structure, as observed in the UV-visible spectra. The addition of imidazole or 2-methylimidazole caused a hypochromic effect in the Soret bands and an initial hyperchromic effect followed by a hypochromic effect in the Q bands, suggesting the formation of tetragonal complexes and a decrease in π-bonding. These findings indicate a transition in the geometry of manganese(III) pyridyl porphyrin from octahedral to tetragonal complexes with successive additions of primary amine, imidazole or 2-methylimidazole. The cyclic voltammogram also confirmed the alteration in geometry, indicating changes in the redox properties of the compound. The redox processes observed in $Mn(Py)_4P$ provide an understanding of its electron-rich porphyrin nature, which destabilizes the manganese(II) oxidation state.

CONFLICT OF INTEREST

The authors declare that there is no conflict of interests regarding the publication of this article.

REFERENCES

1. K.M. Smith, Porphyrins In: J.A. McCleverty and T.J. Meyer, Comprehensive Coordination Chemistry II, Pergamon, p. 493 (2003); https://doi.org/10.1016/B0-08-043748-6/01050-1
2. S.G. Afonso, R. Enríquez de Salamanca and A.M.C. Batlle, *Braz. J. Med. Biol. Res.*, **32**, 255 (1999); https://doi.org/10.1590/S0100-879X1999000300002
3. Z. Liu, H. Li, Z. Tian, X. Liu, Y. Guo, J. He, Z. Wang, T. Zhou and Y. Liu, *ChemPlusChem*, **87**, e202200156 (2022); https://doi.org/10.1002/cplu.202200156
4. N. Tsolekile, S. Nelana and O.S. Oluwafemi, *Molecules*, **24**, 2669 (2019); https://doi.org/10.3390/molecules24142669
5. C.-Y. Huang, W.-L. Yeh and S.-H. Cheng, *J. Electroanal. Chem.*, **577**, 179 (2005); https://doi.org/10.1016/j.jelechem.2004.11.029
6. K.D. Borah and J. Bhuyan, *J. Coord. Chem.*, **72**, 2251 (2019); https://doi.org/10.1080/00958972.2019.1654092
7. L. Xu, H. Lei, Z. Zhang, Z. Yao, J. Li, Z. Yu and R. Cao, *Phys. Chem. Chem. Phys.*, **19**, 9755 (2017); https://doi.org/10.1039/C6CP08495H
8. A.T. Singh and A. Lemtur, *Spectrochim. Acta A Mol. Biomol. Spectrosc.*, **59**, 1549 (2003); https://doi.org/10.1016/S1386-1425(02)00333-5
9. J. Subramanian, V.P. Shedbalkar, A. Lemtur, R. Chakravorty and T.N. Saloi, *J. Phys. Chem.*, **100**, 4770 (1996); https://doi.org/10.1021/jp9511820
10. A. Murugan, V. Thandiayyakone, S. Kumarasamy, C.R. Ravikumar, S. Muthaiah, M. Chakrabarty, P.T. Arasu, T. Rajkumar and H.S. Yadav, *Asian J. Chem.*, **33**, 26 (2020); https://doi.org/10.14233/ajchem.2021.22905
11. V. Thandiayyakone, A. Murugan, C.R. Ravikumar, T. Rajkumar, P. Thillai Arasu, H.S. Yadav and P. Kotteeswaran, *Mater. Today Proc.*, **47**, 933 (2021); https://doi.org/10.1016/j.matpr.2021.04.621
12. M. Liu and Y.O. Su, *J. Electroanal. Chem.*, **426**, 197 (1997); https://doi.org/10.1016/S0022-0728(96)04968-6
13. V. Thandiayyakone, A. Murugan, C.R. Ravikumar, T. Rajkumar and H.S. Yadav, *Res. J. Chem. Environ.*, **26**, 8 (2022); https://doi.org/10.25303/2606rjce08014
14. D.P. Goldberg, A.G. Montalban, A.J.P. White, D.J. Williams, A.G.M. Barrett and B.M. Hoffman, *Inorg. Chem.*, **37**, 2873 (1998); https://doi.org/10.1021/ic970624e
15. M. Paramaguru, A. Murugan, E.R. Nagarajan, S. Kumarasamy, A. Manohar and A. Lemtur, Proceedings of National Seminar on Technologically Important Crystalline and Amorphous Solid (TICAS-2012), Department of Physics, Kalasalingam University, Krishnankoil, India, pp. 103-104, (2012).
16. P. Tagliatesta, J. Li, M. Autret, E. Van Caemelbecke, A. Villard, F. D'Souza and K.M. Kadish, *Inorg. Chem.*, **35**, 5570 (1996); https://doi.org/10.1021/ic960148c
17. A. Murugan, E.R. Nagarajan, A. Manohar, A. Kulandaisamy, A. Lemtur and L. Muthulaksmi, *Int. J. Chemtech Res.*, **5**, 1646 (2013).
18. V. Thandiayyakone, A. Murugan, C.R. Ravikumar, T. Rajkumar, A. Kulandaisamy, I.U. Muzaddadi, A. Manohar, P.T. Arasu and M. Chakrabarty, *Asian J. Chem.*, **35**, 1341 (2023); https://doi.org/10.14233/ajchem.2023.27796
19. N.M. Berezina, M.E. Klueva and M.I. Bazanov, *Macroheterocycles*, **10**, 308 (2017); https://doi.org/10.6060/mhc170507b
20. Z. Valicsek and O. Horvath, *Microchem. J.*, **107**, 47 (2013); https://doi.org/10.1016/j.microc.2012.07.002